Surface diffusion of single vacancies on Ge(111)-$c(2\times8)$ studied by variable temperature scanning tunneling microscopy

I. Brihuega, O. Custance, and J. M. Gómez-Rodríguez*
Departamento de Física de la Materia Condensada, C-III, Universidad Autónoma de Madrid, E-28049-Madrid, Spain
(Received 23 March 2004; published 15 October 2004)

The dynamics of single vacancies on Ge(111)-$c(2\times8)$ surfaces have been investigated by means of variable temperature scanning tunneling microscopy (STM). These vacancies were deliberately created with the STM at different sample temperatures by slight tip-sample contacts. The activation energies and the preexponential factors for the surface diffusion of the created vacancies have been measured, finding that it is a thermally activated motion that presents a slight anisotropic behavior. The activation energy barrier obtained along the $[1\bar{1}0]$ direction is $E_{dy}=0.83\pm0.03$ eV, while along $[\bar{1}\bar{1}2]$ it is $E_{dx}=0.95\pm0.04$ eV. The origin of such anisotropy is discussed in terms of previous experimental results measured only at room temperature as well as previous first-principle calculations of the pristine Ge(111)-$c(2\times8)$ surface. Finally, the vacancy extraction procedure has been investigated in a wide temperature range and it is shown for the first time that it is possible to create single vacancies at temperatures as low as 40 K.

DOI: 10.1103/PhysRevB.70.165410 PACS number(s): 68.35.Fx, 68.35.Dv, 68.37.Ef, 81.16.Ta

I. INTRODUCTION

The diffusion of atomic species on surfaces is one of the most fundamental processes in surface science.[1–6] In particular, it is of crucial importance in the growth and stability of nanostructures on surfaces, an issue of increasing interest for both fundamental and technological reasons. In the last few years, scanning tunneling microscopy (STM) has proven to be a unique tool for the experimental analysis of the diffusion of single adatoms on surfaces. STM is particularly interesting in the case of semiconductor surfaces where a traditional technique for visualizing thermal motion at the atomic scale, i.e., field ion microscopy (FIM),[7] cannot be used. Thus, in the last decade STM has become the technique of choice to measure surface diffusion of single adatoms on semiconductors (see, e.g., Refs. 8–20).

The diffusion of single vacancies on semiconductor surfaces has been relatively less studied by STM.[21–27] This is, however, a very interesting topic as differences with the simpler diffusion of single adsorbates can be expected. For instance, possible charging effects on vacancies leading to changes in the activation energies and preexponential factors for mass transport have been suggested.[28]

The Ge(111)-$c(2\times8)$ surface constitutes a good candidate for surface diffusion analyses on highly reconstructed semiconductor surfaces. On the one hand, despite the complexity of the reconstruction, it is much simpler than another prototypical case, Si(111)-(7×7). On the other hand, the energies involved in mass transport processes on this surface are generally compatible with STM observations at sample temperatures relatively close to room temperature (RT). So, even from the very early developments of variable temperature STM, this system was the choice for studying surface mobility and phase transitions in real time.[29] The diffusion of single adatoms[8,10,30] and molecules[31] has been studied on this surface. It has also been used for STM surface manipulations at the atomic scale[26,32–35] as well as for studies of surface diffusion of STM created artificial vacancies.[27] It is important to stress, however, that these latter previous studies were performed only at room temperature.

As outlined in the previous paragraphs, STM is an ideal tool for the investigation of phenomena that take place at the atomic scale, not only for its ability for viewing objects of atomic size but also because it allows the manipulation of surfaces in a local and controlled way.[26,36,37] In the present work these two remarkable abilities of the STM have been combined. First, a specific region on the surface has been selected, then it has been modified with the STM, and finally some of the dynamical processes that take place due to this modification of the initial surface have been analyzed. More precisely, we have deliberately created single atomic vacancies by slight tip-sample contacts, and studied their diffusion on the Ge(111)-$c(2\times8)$ surface. In this system the motion of the artificially created vacancies over different lattice positions can be observed in real time in a relatively wide temperature range below and above RT, allowing the measurement of the different energy barriers for diffusion existing on this surface. Moreover, the feasibility of controlled atomic modifications in a wider range of sample temperatures has been investigated and it will be shown later that these modifications can be performed at sample temperatures well below RT.

The paper is structured as follows. After this introduction, in Sec. II the experimental setup and the details of sample preparation are presented. In Sec. III A, the main characteristics of the substrate and the procedure for the formation of vacancies with the STM are briefly described. First the thermal mobility of the created vacancies is analyzed in terms of a simple hypothetical isotropic process in Sec. III B. It is then shown that the vacancy diffusion is, indeed, anisotropic. This anisotropy is analyzed and discussed in Sec. III C. Section III D shows the feasibility of the extraction procedure leading to vacancy formation at temperatures much lower than RT. Finally the main conclusions of the present work are summarized in Sec. IV.

II. EXPERIMENTAL DETAILS

The experiments were carried out in an ultrahigh-vacuum (UHV) system whose base pressure is below 5×10^{-11} Torr. The system is equipped with a variable temperature scanning tunneling microscope (VT-STM), low energy electron diffraction (LEED), Auger electron spectroscopy (AES), sample and STM tip transfer and heating capabilities, an STM tip cleaning system by field emission, several interchangeable evaporation cells, a quartz-crystal microbalance, and an ion gun for sample cleaning purposes.

Clean reconstructed Ge(111)-$c(2\times8)$ surfaces were prepared from *n*-type samples (resistivity $\leqslant0.4\ \Omega$ cm) by successive cycles of argon sputtering (beam energy=500 eV, sample current $\sim3-5\ \mu$A, Ar pressure=5×10^{-5} Torr) and annealing ($\sim600°$C) repeated until very sharp and bright $c(2\times8)$ LEED patterns were obtained. The samples were then transferred to the VT-STM and slowly cooled down or heated up to the desired temperature.

The STM experiments were performed with a home-built variable temperature instrument described elsewhere.[20,38] This VT-STM, connected to a continuous flow liquid He UHV cryostat, allows imaging at sample temperatures in the range of 40 to 400 K (the sample temperature can be increased above RT by heat radiation coming from a filament located below the sample holder). STM data were acquired with a fully automated workstation that incorporates digital feedback control based on digital signal processor (DSP) technology.[39] All the surface manipulation experiments, data acquisition, and image processing were performed using the WSXM software.[40] STM images were all acquired in the constant current mode.

III. RESULTS AND DISCUSSION

A. Ge(111)-$c(2\times8)$ surface and vacancy creation procedure

The equilibrium structure of the Ge(111) surface is the well-known $c(2\times8)$ reconstruction. Figure 1(a) represents a schematic of the currently accepted atomic model. For the establishment of this model the first STM images of this surface measured by Becker *et al.*[41,42] were of fundamental importance. As confirmed afterwards by other experimental techniques such as surface x-ray diffraction[43] as well as first-principles calculations,[44] the Ge(111)-$c(2\times8)$ surface consists of adatoms, bonded on T_4 sites to first-layer atoms, and restatoms (first-layer atoms not bonded to adatoms). In Figs. 1(b) and 1(c) typical occupied and empty state STM images, simultaneously measured on this surface, are shown. Due to charge transfer from the adatoms to the restatoms,[44] only the adatoms are visible in empty-state STM images [Fig. 1(c)]. Since the present work is focused on the dynamics of single vacancies, i.e., the absence of an adatom, and the latter are clearly resolved in empty-state images, most of the present measurements were performed at positive sample polarity and, in the following, only empty-state STM images will be shown.

The following procedure was used in order to create single vacancies for the diffusion analysis. First, wide well reconstructed areas of Ge(111)-$c(2\times8)$ with a low density

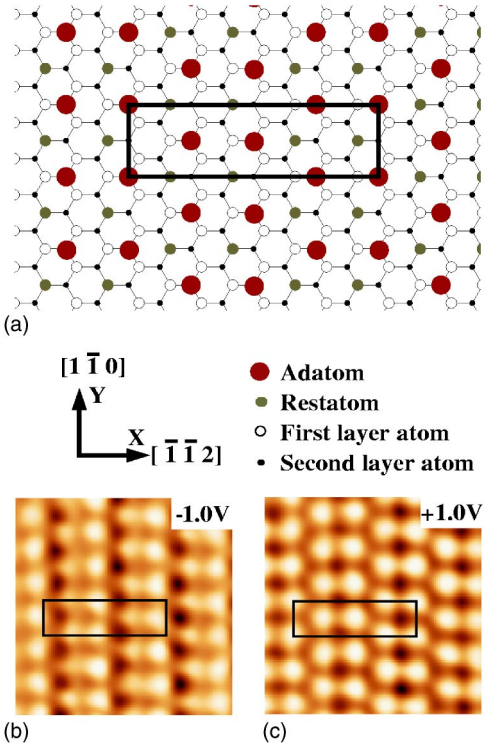

FIG. 1. (Color online) (a) Top view of the atomic model for the Ge(111)-$c(2\times8)$ reconstruction. (b) and (c) 4.8×4.8 nm^2 occupied (−1.0 V) and empty (1.0 V) state STM images. The tunneling current is 1.0 nA for both images.

of natural occurring defects[45,46] were selected. Then a given adatom in this area was chosen and the STM tip was stopped just above it under usual tunneling conditions (bias voltage=+1.0 V and tunneling current=0.5 nA). To create a single vacancy the procedure already reported by Dujardin *et al.*[32] was used. With the tip above the selected adatom, the feedback loop was opened and the bias voltage was set to zero. The tip was then brought towards the sample at a constant rate to a distance of typically 0.6 nm in a time of 20 ms. The tip was held at that position for 20 ms and then retracted back, again at a constant rate, for another 20 ms. Finally the feedback loop was closed, returning to the initial tunneling conditions. An example of one of our nanomanipulation experiments leading to the extraction of a single adatom from the surface is shown in Fig. 2. The STM image in Fig. 2(b) was measured just before the extraction, while Fig. 2(c) was measured, under the same tunneling conditions as the previous one,after the extraction procedure described above was applied. This single vacancy was created at a sample temperature slightly below RT (T=283 K).

B. Thermal diffusion of single vacancies: Isotropic analysis

Once the single vacancy has been created, its evolution is followed by means of STM movies, i.e., series of successive STM images measured on the same surface region. In order to scan the same region for long enough times, residual thermal drifts are corrected in real time by a procedure described elsewhere.[12] All the movies were measured with a sample

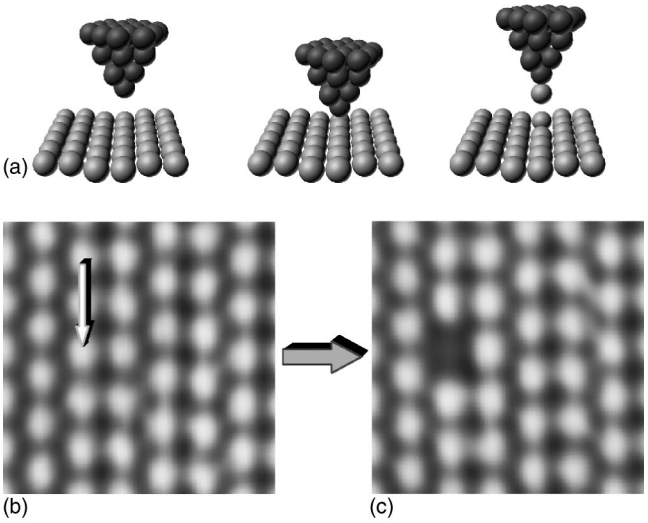

FIG. 2. (a) Schematic representation of the extraction procedure of a single Ge adatom. (b) 4.0×4.0 nm^2 constant current image showing a region just before the manipulation. (c) Same region measured immediately after the creation of the single vacancy. Both (b) and (c) are measured under the same tunneling conditions: sample bias: +1.0 V and tunneling current: 0.5 nA.

bias of 1.0 V and with a tunneling current of 0.5 nA; under these tunneling conditions the STM tip does not influence the vacancy movement.[26] To follow the vacancy motion, its position is registered with respect to the initial one, i.e., the position that it was occupying when the STM movie started just after generating the vacancy. The fact that the vacancy diffuses between well-known lattice positions[47] has been taken into account in order to easily track its exact location as a function of time. Thus, (x,y) coordinates have been assigned to the vacancy position at a given time, where x corresponds to the direction $[\bar{1}\bar{1}2]$ (perpendicular to the adatom rows) and y corresponds to the direction $[1\bar{1}0]$ (parallel to the adatom rows).

Figures 3(a)–3(d) show four frames extracted from an STM movie in which the diffusion of an artificially generated single vacancy over different lattice sites can be observed. The net displacement of the vacancy $[\Delta r=(x^2+y^2)^{1/2}]$ with respect to the initial position $(0,0)$ as a function of time has been outlined. In the course of the present experiments, diffusion events have been observed where a single vacancy splits into two so-called semivacancies, in agreement with the measurements performed at RT by Mayne *et al.*[27] An example of such a situation can be resolved in Fig. 3(d). These semivacancies, separated by a variable number of Ge adatoms in metastable T_4 positions, [26] also diffuse and eventually merge again into a single vacancy. In order to quantify the movement of such semivacancies, in these cases Δr was computed by considering the middle point of the line connecting the positions of both semivacancies, i.e., $x=(x_1+x_2)/2$ and $y=(y_1+y_2)/2$, (x_1,y_1) and (x_2,y_2) being the coordinates of each semivacancy. A scattered plot of all the positions occupied by the vacancy during the whole movie is shown in Fig. 3(e). As can be observed, this plot is reminiscent of the typical pattern of a two-dimensional random walk.

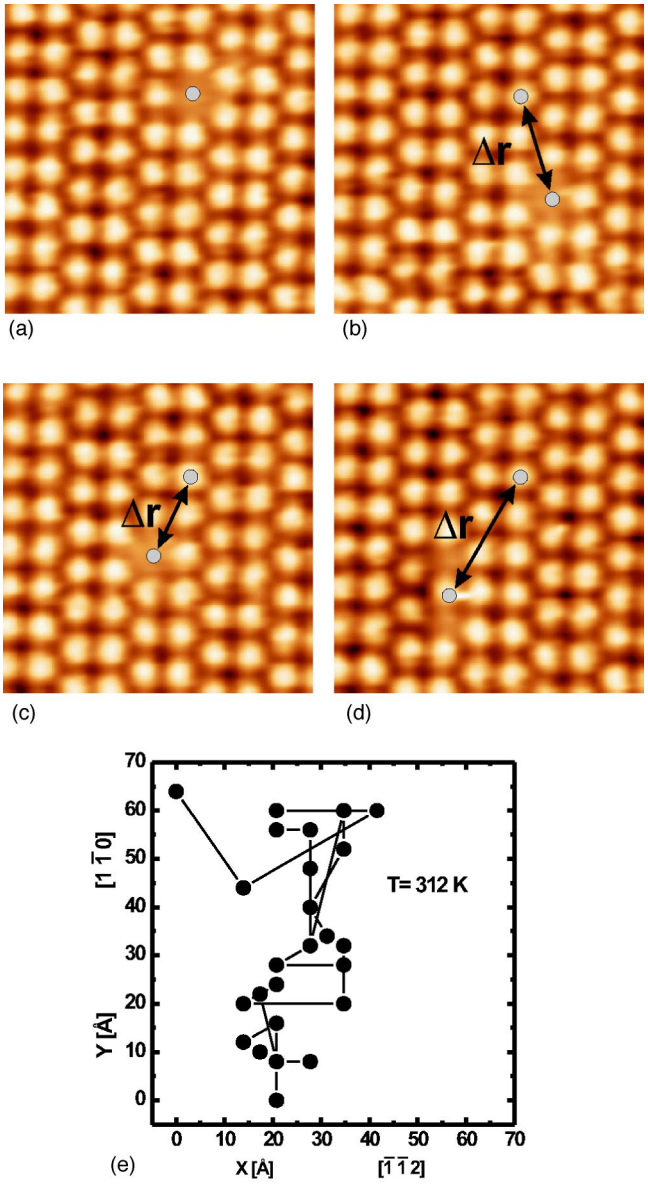

FIG. 3. (Color online) (a) to (d) Series of images extracted from an STM movie measured at 312 K. The arrows show the vacancy displacement (Δr) with respect to the initial position for different times: (a) $t=0$; (b) $t=108$ s, (c) $t=135$ s, (d) $t=180$ s. Size of the images: 6.0×6.0 nm^2; sample bias +1.0 V, tunneling current: 0.5 nA. (e) Plot of all the positions occupied by the vacancy during the movie [the region scanned in the movie was larger than the one shown in (a) to (d)]. Movie length: 405 s; number of frames: 45.

In order to verify this qualitative picture, the mean square displacement $\langle\Delta r^2\rangle$ must be computed by measuring and averaging over a large number of movies like the one shown in Fig. 3. For a random walk motion, this quantity must increase linearly with time. Then, using the Einstein relation $\langle\Delta r^2\rangle=2dDt$ (d being the dimension, i.e., $d=2$ for surface diffusion), the diffusion coefficient D for a given temperature can, in principle, be measured. In order to confirm that the vacancy motion is thermally activated and to obtain its activation energy as well as the preexponential factor, it is necessary to perform the experiments at different sample tem-

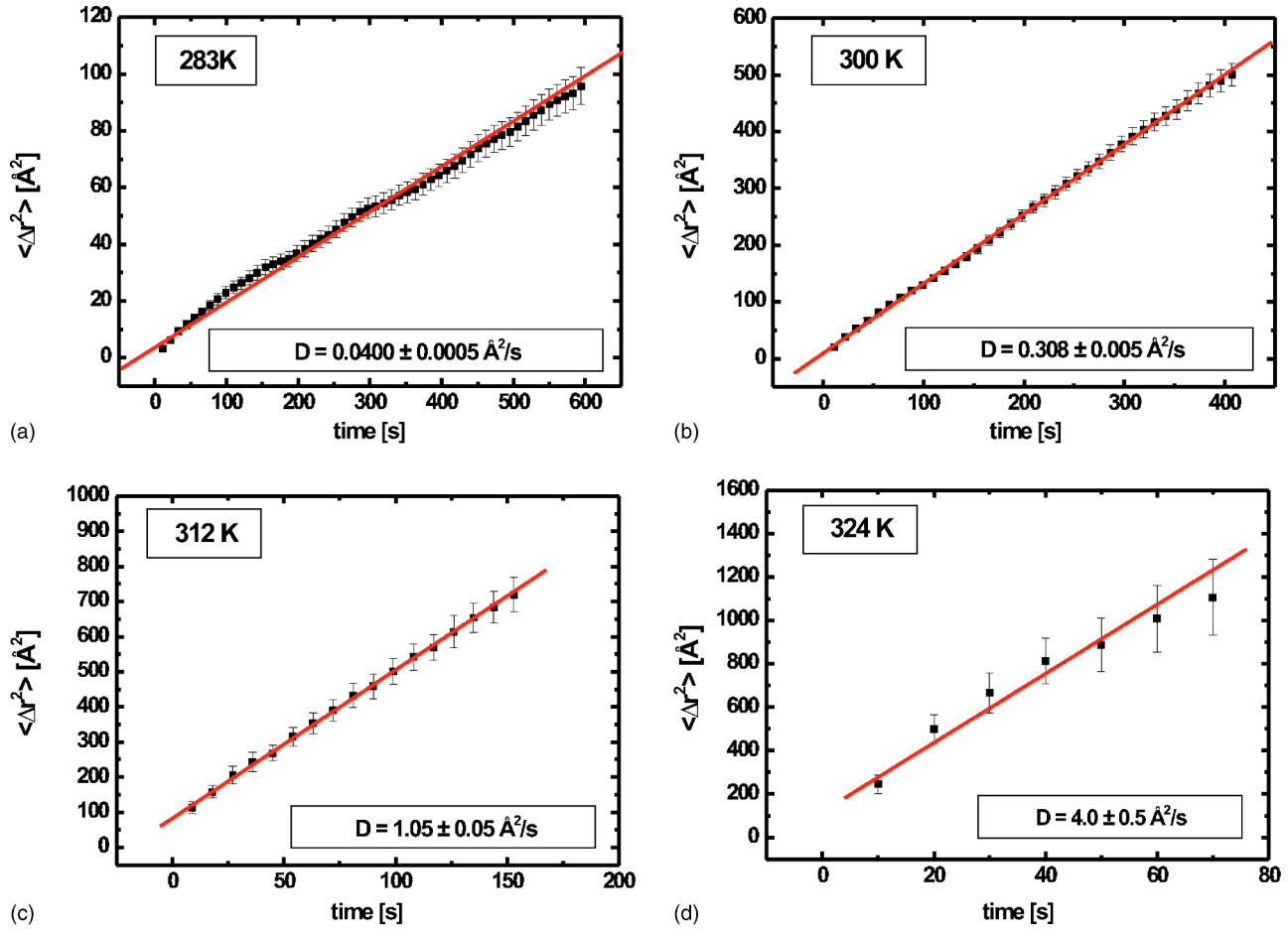

FIG. 4. (Color online) (a) to (d) Plots of the mean square displacement ($\langle \Delta r^2 \rangle$) of the vacancy *versus* time. For each sample temperature, $\langle \Delta r^2 \rangle$ is the average of a large number of STM movies (see text for detailed explanation). The diffusion coefficients D for each temperature are obtained from the slopes of each figure: $\langle \Delta r^2 \rangle = 2dDt$ (with $d=2$).

peratures. As is well known, for thermally activated motion the diffusion coefficient D must follow an Arrhenius expression of the form $D=D_0 \exp(-E_d/kT)$, where E_d is the effective energy barrier, k is the Boltzmann constant, and D_0 is the diffusion constant or preexponetial factor. In the present experiments vacancy motion can be observed with STM at RT. Therefore, all the experiments have been performed in a temperature range around RT (between 280 and 325 K).

In Figs. 4(a)–4(d) the experimentally measured mean square displacements $\langle \Delta r^2 \rangle$ as a function of time for different sample temperatures are plotted. In order to get good statistics in the experimental determination of $\langle \Delta r^2 \rangle$ the following method, inspired in early field ion microscopy (FIM) works,[48] was used. First, for a given temperature a large data set of STM movies was measured, all of the movies being recorded at the same rate (typically 1 frame every 10 s at RT). As the vacancy jumps are independent of each other, to get the mean square displacement $\langle \Delta r^2 \rangle$ for a given time, all the possible intervals between frames corresponding to this particular time lapse in each movie were considered (i.e., if a particular time interval of 40 s and a frame rate of 10 s/frame are chosen just for illustrative purposes, then Δr^2 would be measured considering frames 1,5,9,13, … and 2,6,10,14, … and so on). A clear linear dependency of the mean square displacement on time can be deduced from Fig. 4 for all the temperatures that have been analyzed. The corresponding diffusion coefficients for each of these temperatures have been obtained from the slope of the linear fit to the experimental data shown in Figs. 4(a)–4(d). Figure 5 shows the Arrhenius plot obtained by representing the D values as a function of the inverse temperature. From the excellent fit of the diffusion coefficient in the Arrhenius plot it can be concluded that the vacancy motion is a thermally activated process, with an effective energy barrier $E_d = 0.88 \text{ eV} \pm 0.02 \text{ eV}$. This value is in very good agreement with the value estimated from measurements performed only at RT by Mayne *et al.*[27] (0.88–0.90 eV). Moreover, the experimental value obtained in the present experiments for the preexponential factor is $D_0 = 10^{14.3 \pm 0.3}$ Å^2/s, a value which is within the range of what is usually considered as normal in simple surface diffusion of single adatoms.[7]

C. Anisotropy in the diffusion process

All the analysis shown in the previous section is based on a simple isotropic diffusion model for single vacancies on Ge(111)-$c(2\times8)$ surfaces.[27] Some doubts, however, can be cast on the isotropic character of this process just by simple

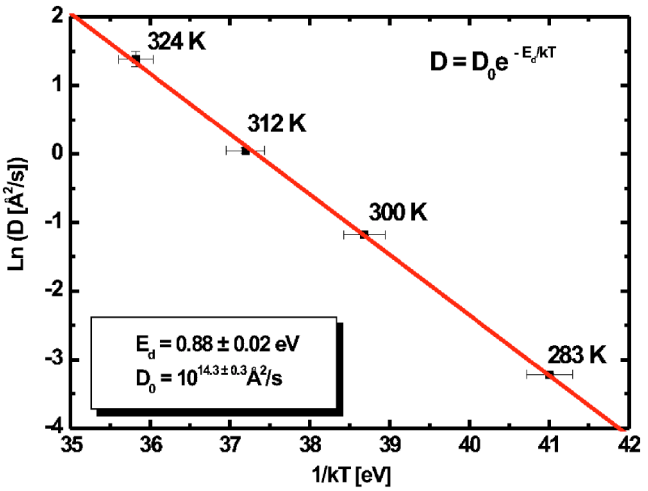

FIG. 5. (Color online) Arrhenius plot for the diffusion coefficent D. The effective activation energy barrier (E_d) and the preexponential factor (D_0) are obtained from the best fit to the Arrhenius expression (represented by the solid line).

inspection of the scattered plots displaying the sites visited by a single vacancy during a long enough STM movie. An example of this can be observed in Fig. 3(e), where the motion of the vacancy is much more extended in the vertical direction than in the perpendicular one. This is the typical behavior of all the movies that have been recorded. Moreover, from previous experimental observations of the pristine Ge(111)-$c(2\times8)$ surface by Feenstra *et al.*[29,49] and Hwang *et al.*, [10] it has been suggested that Ge adatom diffusion on this surface should be anisotropic, it being easier for the original adatoms of the reconstruction to move along the $[\bar{1}10]$ direction (y), parallel to adatom rows, than to move along the $[\bar{1}\bar{1}2]$ direction (x), perpendicular to adatom rows. This anisotropy is consistent with first-principles calculations performed on the perfect surface (with no vacancies) by Takeuchi *et al.*[47] Regarding the diffusion of single vacancies on this surface, there is, to our best knowledge, only one previous experimental study performed at RT, where the anisotropy issue was not addressed.[27] From the theoretical viewpoint, up to date there exists no first-principles calculation where single vacancies have successfully been generated on this surface.

In order to clarify this important point, in the present work a separate study for the vacancy diffusion along each direction has been undertaken. The way of procedure was analogous to that presented in the previous section, but considering the vacancy motion as two independent one-dimensional random walks along x and y directions. In Fig. 6 the experimental results for the mean square displacement along each direction as a function of time measured at RT are displayed. The most remarkable feature in this figure is that at RT the diffusion coefficient along $[\bar{1}10]$ is more than twice the value obtained along $[\bar{1}\bar{1}2]$, i.e., the diffusion processes leading to single vacancy migration on the surface are clearly anisotropic.[50]

In order to go on with the quantitative analysis, the diffusion coefficients were measured independently for the x and

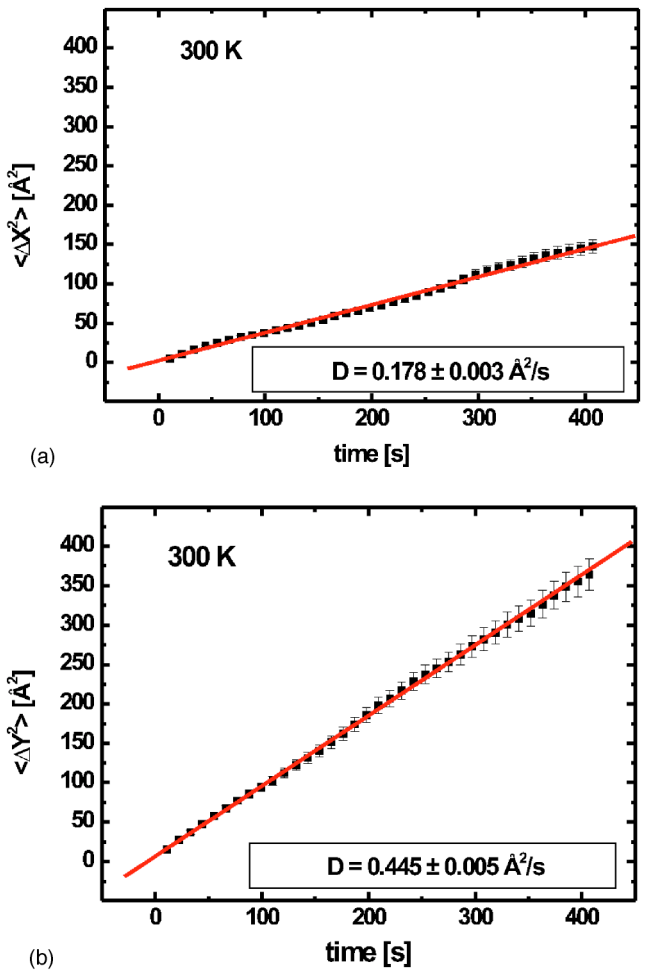

FIG. 6. (Color online) (a) and (b) Plots of the mean square displacement of the vacancy along x ($[\bar{1}\bar{1}2]$) and y ($[\bar{1}10]$), respectively, as a function of time. In both cases the diffusion coefficients are obtained from the Einstein relation for a one-dimensional random walk $\langle\Delta r^2\rangle = 2Dt$.

y directions in the same temperature range as that used in the previous section (280 to 325 K). In Fig. 7 Arrhenius plots corresponding to each direction are shown. As can be deduced from this figure, the anisotropic behavior takes place for the whole range of temperatures measured in the present work. The activation energy barrier obtained for single vacancy migration along the direction parallel to the adatom rows ($E_{dy}=0.83\pm0.03$ eV) is clearly smaller than the activation energy obtained for the perpendicular direction to them ($E_{dx}=0.95\pm0.04$ eV). These measurements represent, to our knowledge, the first experimental quantitative confirmation of the anisotropy of single vacancy diffusion on the Ge(111)-$c(2\times8)$ surface.

The origin of such anisotropic behavior is not simple. As has already been stated, anisotropy in adatom diffusion on perfect Ge(111)-$c(2\times8)$ surfaces had already been detected qualitatively in previous experiments.[10,29,49] By means of first-principles density functional theory calculations it was suggested [47] that the origin of the anisotropy on the perfect surface could be twofold. On the one hand, the most favorable diffusion paths for Ge adatoms are those connecting T_4

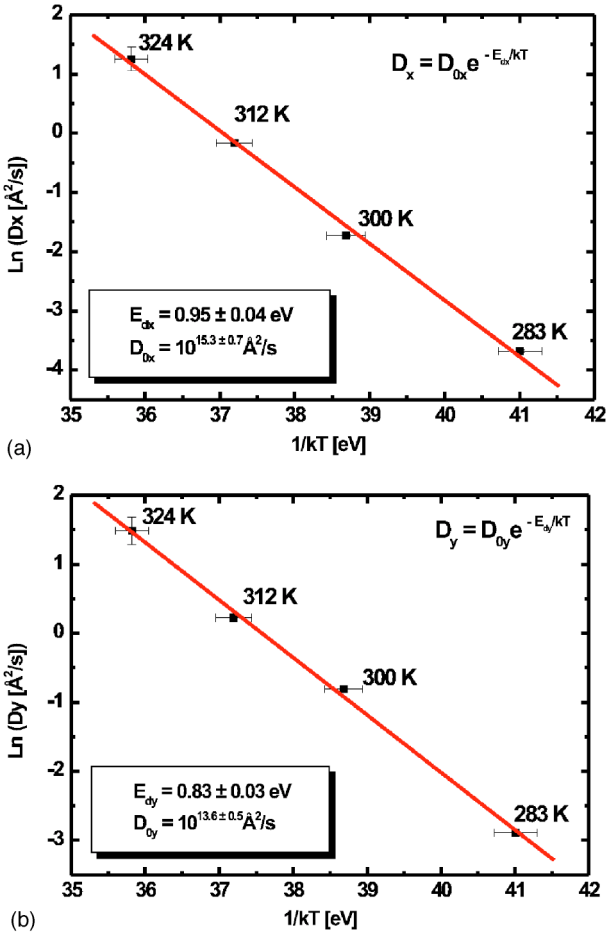

FIG. 7. (Color online) Arrhenius plots for the diffusion coefficient along (a) x ($[\bar{1}12]$) and (b) y ($[\bar{1}10]$). The activation energies (E_{dx} and E_{dy}) and the preexponential factors (D_{0x} and D_{0y}) for each direction are obtained from the best fit to the Arrhenius expressions (represented by the solid lines) from the corresponding plots.

sites with H_3 sites. However, for one out of the two adatoms in the unit cell, i.e., the adatom which is surrounded by four restatoms, one of the three H_3 sites, the one along $[\bar{1}12]$, is much higher in energy. This feature, originating from the special topology of the reconstruction, appeared to be the main reason for the anisotropy of adatom diffusion. On the other hand, it was found that diffusing adatoms tend to be very correlated along $[1\bar{1}0]$ and that the most likely diffusion mechanism along this direction was the correlated jump of several Ge adatoms together. On the contrary, correlated jumps along the perpendicular direction $[\bar{1}12]$ were completely discarded. Although, all the calculations were performed on a surface free of adatom vacancies, it was also suggested by the authors that in the presence of them the situation could be substantially different, the most likely diffusing mechanism being a simple uncorrelated motion where Ge adatoms would hop one by one along the adatom row.

In the present experiments, in describing the anisotropy in diffusion an orthogonal coordinate system has been chosen, a fact that is justified by the diagonal character of the two-dimensional diffusion tensor that has been calculated.[50] This analysis is directly related to the overall mass transport, which presents clear anisotropic behavior. However, a direct comparison of the extracted barriers for diffusion along each direction and atomic scale events is not straightforward, as individual vacancy hops can involve simultaneous movements along x and y. This means that the extracted barriers have to be seen as average values when compared to atomic-scale events. In this sense, the measured average diffusion barrier for migration along the most favorable direction $[1\bar{1}0]$ has a value ($E_{dy}=0.83\pm0.03$ eV) which is in extraordinarily good agreement with that calculated by Takeuchi *et al.*[47] for correlated diffusion of Ge adatoms of the perfect surface along this direction (0.8 eV). The average diffusion barrier measured along the perpendicular direction ($E_{dx}=0.95\pm0.04$ eV) is, however, somehow smaller than that expected from the calculations on the perfect surface (larger than 1.0 eV).[51]

The comparison of the barriers measured along the two perpendicular directions with those obtained from first-principles calculations on the perfect surface would tend to suggest that the existence of long jumps of adatom vacancies along the adatom rows (or what it is equivalent, the existence of correlated jumps of adatoms) may be responsible for the observed anisotropy, as it is well known that the existence of non-nearest-neighbor jumps in one particular direction, and not in another one, can be the origin of anisotropy on other surfaces.[52] In the present experiments, however, such correlated jumps along $[1\bar{1}0]$ have not been detected unambiguously. Nevertheless, it has been repeatedly observed that the formation of semivacancies separated by one or more Ge adatoms [see Fig. 3(d)] could be related to the anisotropy issue. Although these semivacancies do correspond to metastable states,[26] it has been detected in the whole temperature range reported here that they are much more mobile than single vacancies. For instance, at 300 K, the probability of observing a diffusion event of a semivacancy is approximately three times larger than the probability corresponding to a single vacancy (77% versus 28%). Due to the special configuration of the reconstruction, once the semivacancies are formed, they can move separately along the adatom rows, a situation that cannot happen along the perpendicular direction to these adatom rows.[26] This makes it possible that the semivacancies can diffuse independently to longer distances along $[1\bar{1}0]$ than along $[\bar{1}12]$. This fact, combined with the higher mobility of the semivacancies mentioned above, tends to favor the motion along $[1\bar{1}0]$, and therefore the anisotropy of the diffusion.

Although the present work quantitatively demonstrates the anisotropy in adatom vacancy diffusion, it has to be taken into account that the analysis presented here is based on average values extracted from mean square displacement measurements. A precise determination of the atomistic origin of the anisotropy in the presence of vacancies should rely on a full quantitative description of all the possible diffusing events at the atomic scale on this surface. This analysis would need to account for the existence of different metastable and stable adsorption sites and different energy barriers along different directions.[53] This represents a formidable

task that has never been undertaken on such complicated systems and is completely out of the scope of the present work.

D. Low-temperature creation of vacancies

A last issue that is addressed in the present work is the feasibility of creating single vacancies in a wide range of sample temperatures. In previous works this process was only performed at RT and, as it has been described above, at this temperature single vacancies diffuse between different lattice positions. Here our main focus was on the low temperatue regime (i.e., below RT) since, as it is a thermally activated process, if the sample temperature is lowered enough, the vacancy motion should slow down and even stop. This could open the possibility of creating permanent modifications on the surface at these low temperatures. In the present experiments it has been possible to create single vacancies at temperatures above RT, and what is more important at temperatures far below RT. More precisely it has been possible to successfully perfom the extraction procedure at temperatures as low as 40 K (i.e., approximately the minimum attainable temperature with our experimental setup). As one would expect, at such low temperatures these vacancies remain completely trapped and they do not diffuse anymore. Figure 8 shows the result of one of these experiments in which a single adatom vacancy was created at 40 K. Dujardin *et al.*[32] have discussed the mechanism for the extraction of individual atoms from the Ge(111)-$c(2\times8)$ surface with the STM tip. According to their calculations, at zero bias voltage, when the tip and sample approach closely enough, a collapse of the energy barrier for the adatom of the surface to migrate to the tip apex can occur. The possibility of extracting adatoms at temperatures as low as the one reported in the present work seems to indicate that the mechanism proposed by these authors is still valid at such low temperatures.

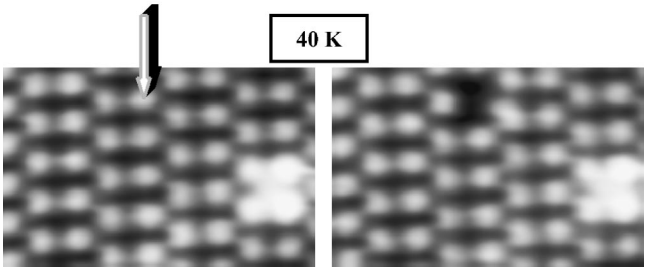

FIG. 8. Example of the creation of a single vacancy at 40 K. Once the vacancy was created it remained fixed in the same position. Size of the images: 5.5×4.0 nm^2; sample bias: +1.0 V, tunneling current: 0.5 nA.

IV. CONCLUSIONS

To summarize, the dynamics of single vacancies in the Ge(111)-$c(2\times8)$ surface created with the STM tip itself by gentle tip-sample contacts have been studied. The diffusion of such vacancies in a temperature range between 280 and 325 K has been analyzed, demonstrating that it is a thermally activated motion. A slight anisotropic behavior has been detected: the vacancies have higher mobility (and thus a smaller activation energy barrier, $E_{dy}=0.83$ eV) along the parallel direction to the adatom rows than in the perpendicular direction to them ($E_{dx}=0.95$ eV). Finally it has been shown that single vacancies can be created at temperatures as low as 40 K where they remain motionless. This opens the possibility for future nanopatterning of this surface at the atomic scale.

ACKNOWLEDGMENTS

We thank J. M. Soler for fruitful discussions and B. Power for critical reading of the manuscript. Financial support from Spain's MCyT under Grant No. BFM2001-0186 is gratefully acknowledged.

*Corresponding author. Email address: josem.gomez@uam.es

[1] E. G. Seebauer and C. E. Allen, Prog. Surf. Sci. **49**, 265 (1995).
[2] T. R. Linderoth, S. Horch, E. Lægsgaard, I. Stensgaard, and F. Besenbacher, Phys. Rev. Lett. **78**, 4978 (1997).
[3] H. Brune, Surf. Sci. Rep. **31**, 121 (1998).
[4] J. V. Barth, Surf. Sci. Rep. **40**, 75 (2001).
[5] T. T. Tsong, Prog. Surf. Sci. **67**, 235 (2001).
[6] T. Ala-Nissila, R. Ferrando, and S. C. Ying, Adv. Phys. **51**, 949 (2002).
[7] G. L. Kellog, Surf. Sci. Rep. **21**, 88 (1994).
[8] E. Ganz, S. K. Theiss, I. S. Hwang, and J. Golovchenko, Phys. Rev. Lett. **68**, 1567 (1992).
[9] Y. W. Mo, Phys. Rev. Lett. **71**, 2923 (1993).
[10] I. S. Hwang, S. K. Theiss, and J. Golovchenko, Science **265**, 490 (1994).
[11] C. Pearson, B. Borovsky, M. Krueger, R. Curtis, and E. Ganz, Phys. Rev. Lett. **74**, 2710 (1995).
[12] J. M. Gómez-Rodríguez, J. J. Saenz, A. M. Baró, J. Y. Veuillen, and R. C. Cinti, Phys. Rev. Lett. **76**, 799 (1996).
[13] B. S. Swartzentruber, Phys. Rev. Lett. **76**, 459 (1996).
[14] B. C. Stipe, M. A. Rezaei, and W. Ho, Phys. Rev. Lett. **79**, 4397 (1997).
[15] R. L. Lo, I. S. Hwang, M. S. Ho, and T. T. Tsong, Phys. Rev. Lett. **80**, 5584 (1998).
[16] T. Hitosugi, Y. Suwa, S. Matsuura, S. Heike, T. Onogi, S. Watanabe, T. Hasegawa, K. Kitazawa, and T. Hashizume, Phys. Rev. Lett. **83**, 4116 (1999).
[17] T. Sato, S. Kitamura, and M. Iwatsuki, J. Vac. Sci. Technol. A **18**, 960 (2000).
[18] O. Custance, I. Brihuega, J. M. Gómez-Rodríguez, and A. M. Baró, Surf. Sci. **482**, 1406 (2001).
[19] V. Cherepanov and B. Voigtländer, Appl. Phys. Lett. **81**, 4745 (2002).
[20] O. Custance, S. Brochard, I. Brihuega, E. Artacho, J. M. Soler, A. M. Baró, and J. M. Gómez-Rodríguez, Phys. Rev. B **67**, 235410 (2003).

[21] N. Kitamura, M. G. Lagally, and M. B. Webb, Phys. Rev. Lett. **71**, 2082 (1993).
[22] P. Ebert, M. G. Lagally, and K. Urban, Phys. Rev. Lett. **70**, 1437 (1993).
[23] X. Chen, F. Wu, Z. Zhang, and M. G. Lagally, Phys. Rev. Lett. **73**, 850 (1994).
[24] G. Lengel, J. Harper, and M. Weimer, Phys. Rev. Lett. **76**, 4725 (1996).
[25] P. Ebert, X. Chen, M. Heinrich, M. Simon, K. Urban, and M. G. Lagally, Phys. Rev. Lett. **76**, 2089 (1996).
[26] P. Molinàs-Mata, A. J. Mayne, and G. Dujardin, Phys. Rev. Lett. **80**, 3101 (1998).
[27] A. J. Mayne, F. Rose, C. Bolis, and G. Dujardin, Surf. Sci. **486**, 226 (2001).
[28] H. Yeung, H. Chan, K. Dev, and E. G. Seebauer, Phys. Rev. B **67**, 035311 (2003).
[29] R. M. Feenstra, A. J. Slavin, G. A. Held, and M. A. Lutz, Phys. Rev. Lett. **66**, 3257 (1991).
[30] Z. Gai, H. Yu, and W. S. Yang, Phys. Rev. B **53**, 13 547 (1996).
[31] K. R. Wirth and J. Zegenhagen, Phys. Rev. B **56**, 9864 (1997).
[32] G. Dujardin, A. Mayne, O. Robert, F. Rose, C. Joachim, and H. Tang, Phys. Rev. Lett. **80**, 3085 (1998).
[33] G. Dujardin, A. J. Mayne, and F. Rose, Phys. Rev. Lett. **82**, 3448 (1999).
[34] G. Dujardin, F. Rose, J. Tribollet, and A. J. Mayne, Phys. Rev. B **63**, 081305 (2001).
[35] G. Dujardin, F. Rose, and A. J. Mayne, Phys. Rev. B **63**, 235414 (2001).
[36] D. M. Eigler and E. K. Schweizer, Nature (London) **344**, 524 (1990).
[37] L. Bartels, G. Meyer, and K.-H. Rieder, Phys. Rev. Lett. **79**, 697 (1997).
[38] O. Custance, Ph.D. thesis, Universidad Autónoma de Madrid, Madrid, 2002.
[39] Nanotec Electrónica S.L.
[40] WSxM free software downloadable from http://www.nanotec.es.
[41] R. S. Becker, J. A. Golovchenko, and B. S. Swartzentruber, Phys. Rev. Lett. **54**, 2678 (1985).
[42] R. S. Becker, B. S. Swartzentruber, J. S. Vickers, and T. Klitsner, Phys. Rev. B **39**, 1633 (1989).
[43] R. Feidenhans'l, J. S. Pedersen, J. Bohr, M. Nielsen, F. Grey, and R. L. Johnson, Phys. Rev. B **38**, 9715 (1988).
[44] N. Takeuchi, A. Selloni, and E. Tosatti, Phys. Rev. Lett. **69**, 648 (1992).
[45] P. Molinàs-Mata and J. Zegenhagen, Phys. Rev. B **47**, 10 319 (1993).
[46] G. Lee, H. Mai, I. Chizhov, and R. F. Willis, Surf. Sci. **463**, 55 (2000).
[47] N. Takeuchi, A. Selloni, and E. Tosatti, Phys. Rev. B **49**, 10 757 (1994).
[48] G. Ehrlich and F. G. Hudda, J. Chem. Phys. **44**, 1039 (1966).
[49] R. M. Feenstra, A. J. Slavin, G. A. Held and M. A. Lutz, Ultramicroscopy **42-44**, 33 (1992).
[50] In a two-dimensional system, the diffusion tensor can be defined as $\mathbf{D}=\begin{pmatrix} D_{xx} & D_{xy} \\ D_{yx} & D_{yy} \end{pmatrix}$, where $D_{xx}=\langle \Delta x^2 \rangle / 2t$, $D_{yy}=\langle \Delta y^2 \rangle / 2t$ and $D_{xy}=D_{yx}=\langle \Delta x \Delta y \rangle / 2t$. In the present work, two orthogonal axes ($[\bar{1}12]$ and $[1\bar{1}0]$) have been chosen as principal axes and the corresponding components have been calculated. For a sample temperature of 300 K, the components along x and along y are $D_x \equiv D_{xx}=0.178\pm0.003$ Å^2/s and $D_y \equiv D_{yy}=0.445\pm0.005$ Å^2/s (see Fig. 6). The cross term, $D_{xy}=D_{yx}$, has also been computed from the experimental data at 300 K and its value ($D_{xy}=0.012\pm0.003$ Å^2/s) is negligible compared to D_{xx} and D_{yy}. This ensures that the diffusion tensor is diagonal with the chosen basis set.
[51] Although the energy barrier for a T_4-H_3-T_4 uncorrelated diffusion event along $[\bar{1}12]$ is not stated in Ref. 47 , the energy of the local minimum corresponding to this H_3 site is ~1.0 eV (compared to ~0.6 eV for the other two neighbor H_3 sites). Accordingly, the full barrier would be expected to be larger than 1.0 eV.
[52] S. M. Oh, S. J. Koh, K. Kyuno, and G. Ehrlich, Phys. Rev. Lett. **88**, 236102 (2002).
[53] A valuable approximation to this problem has been developed in Ref. 27 . However, this analysis, performed only at RT, relies on the isotropy of the diffusion of single vacancies on Ge(111)-$c(2\times8)$. The inclusion of anisotropies in the equations worked out by these authors would imply such huge experimental statistics that it becomes, in practice, unfeasible for this reconstruction.